Nuclear Magnetic Resonance−Based Dissection of a Glycosyltransferase Specificity for the Mucin MUC1 Tandem Repeat †

ARTICLE *in* BIOCHEMISTRY · JANUARY 2004

Impact Factor: 3.02 · DOI: 10.1021/bi0353070 · Source: PubMed

7 AUTHORS, INCLUDING:

Richard Brokx
University Health Network
16 PUBLICATIONS **294** CITATIONS
SEE PROFILE

Tapas Mal
The Ohio State University
41 PUBLICATIONS **1,569** CITATIONS
SEE PROFILE

Nuclear Magnetic Resonance-Based Dissection of a Glycosyltransferase Specificity for the Mucin MUC1 Tandem Repeat†

Richard D. Brokx, Leigh Revers, Qinghong Zhang, Shaoxian Yang, Tapas K. Mal, Mitsuhiko Ikura, and Jean Gariépy*

Department of Medical Biophysics, University of Toronto, 610 University Avenue, Toronto, Ontario M5G 2M9, Canada

Received July 23, 2003; Revised Manuscript Received September 22, 2003

ABSTRACT: The human glycoprotein MUC1 mucin plays a critical role in cancer progression. Breast, ovarian, and colon cancer cells often display unique cell-surface antigens corresponding to aberrantly glycosylated forms of the MUC1 tandem repeat. In this report, ^{15}N- and ^{13}C-labeled forms of a recombinant MUC1 construct containing five tandem repeats were used as substrates to define the order and kinetics of addition of N-acetylgalactosamine (GalNAc) moieties by a recombinant active form of the human enzyme UDP-GalNAc:polypeptide *N*-acetylgalactosaminyltransferase I (ppGalNAc-T1; residues 40−559). Heteronuclear NMR experiments were performed to assign resonances associated with the two serines (Ser5 and Ser15) and three threonines (Thr6, Thr14, and Thr19) present in the 20-residue long MUC1 repeat. The kinetics and order of addition of GalNAc moieties (Tn antigen) on the MUC1 construct by human ppGalNAc-T1 were subsequently dissected by NMR spectroscopy. Threonine 14 was shown to be rapidly glycosylated by ppGalNAc-T1 with an initial rate of 25 μM/min, followed by Thr6 (8.6 μM/min). The enzyme also modified Ser5 at a slower rate (1.7 μM/min), an event that started only after the glycosylation of Thr14 and Thr6 side chains was mostly completed. Ser15 and Thr19 remained unglycosylated by ppGalNAc-T1. Corresponding O-glycosylation sites within all five tandem repeats were simultaneously modified by ppGalNAc-T1, suggesting that each repeat behaves as an independent substrate unit. This study demonstrated that the hydroxyl oxygens of Thr14 and to a lesser extent Thr 6 represent the two dominant substrates modified by ppGalNAc-T1 within the context of a complex MUC1 peptide substrate. More importantly, the availability of defined isotopically labelled MUC1 glycopeptide substrates and the relative simplicity of their NMR spectra will facilitate the analysis of other transferases within the O-glycosylation pathways and the rational design of tumor-associated MUC1 antigens.

Golgi-resident glycosyltransferases are responsible for the attachment of O-linked oligosaccharide chains to serine and threonine residues of proteins. The initial step in the O-glycosylation pathway involves the transfer of an *N*-acetylgalactosamine (GalNAc)[1] residue from UDP-GalNAc to a protein. This event is catalyzed by a family of enzymes, the UDP-GalNAc:polypeptide *N*-acetylgalactosaminyltransferases (ppGalNAc-transferases) (*1*), of which there are at least 14 isoforms in humans alone (*2*). These ppGalNAc-transferases are differentially expressed, in terms of development and tissue distribution (*3*). The most frequently studied substrate for this class of enzymes is the 20-amino acid long tandem repeat of human mucin MUC1, a glycoprotein that is found on the surfaces of most epithelial cells. Specifically, the extracellular domain of MUC1 consists primarily of a variable number (40−100) of tandem repeats with the sequence PAPGSTAPPAHGVTSAPDTR. This sequence has five potential O-glycosylation sites (three threonine and two serine residues). Interestingly, the MUC1 tandem is aberrantly glycosylated in a variety of cancers (*4*−*7*), with the consequence that tumor cells present MUC1 glycoforms (*4*, *8*) that bear predominantly less elaborate, truncated oligosaccharide side chains compared to normal tissues. The underlying mechanism for this change is widely believed to involve a shift from core 2 ([GlcNAc(β1−6)Gal(β1−3)]GalNAc-(α1-*O*)Ser/Thr) to core 1 [Gal(β1−3)GalNAc(α1-*O*)-Ser/Thr] and shorter oligosaccharide structures (*8*). MUC1-directed antibodies often recognize truncated oligosaccharide structures found within the tandem repeat (*9*−*11*), specifically the Tn [GalNAc(α1-*O*)Ser/Thr], sialyl-Tn [Neu5Ac-(α2−6)GalNAc(α1-*O*)Ser/Thr], T (i.e., core 1), and sialyl-T [Neu5Ac(α2−3)Gal(β1−3)GalNAc(α1-*O*)-Ser/Thr] antigens. These cancer-associated MUC1 epitopes may serve as antigens in the development of cancer vaccines (*6*, *12*).

† This work is funded by grants from the Canadian Breast Cancer Research Alliance and the National Cancer Institute of Canada in association with the Canadian Cancer Society. M.I. is the recipient of a Senior Investigator Award from the Canadian Institutes of Health Research.

* To whom correspondence should be addressed: Phone 416-946-2967; fax 416-946-6529; e-mail gariepy@uhnres.utoronto.ca.

[1] Abbreviations: BSM, bovine submaxillary mucin; CSI, chemical shift index; GalNAc, *N*-acetylgalactosamine; ppGalNAc-T1, uridine-5′-diphospho-*N*-acetylgalactosamine:polypeptide *N*-acetylgalactosaminyltransferase I; HSQC, heteronuclear single quantum coherence spectrum; MES, 2-(*N*-morpholino)ethanesulfonic acid; MUC1-5TR and $GalNAc_3$-MUC1-5TR, protein consisting of five MUC1 tandem repeats preceded by a vector-encoded His_6 tag and the same protein glycosylated at three positions per tandem repeat; NOESY, nuclear Overhauser effect spectroscopy; NTA, nitrilotriacetate; PBS, phosphate-buffered saline; PCR, polymerase chain reaction; SDS−PAGE, sodium dodecyl sulfate−polyacrylamide gel electrophoresis; TOCSY, total correlation spectroscopy; UDP-GalNAc, uridine-5′-diphospho-*N*-acetylgalactosamine.

10.1021/bi0353070 CCC: $25.00
Published on Web 11/04/2003

The general pattern of *O*-glycosylation of the MUC1 repeat by ppGalNAc-transferases had been established in the past by Edman degradation and/or mass spectrometric analysis (*13*−*15*). However, more detailed kinetic studies on the site-specific selectivity of these enzymes for complex substrates such as the MUC1 tandem repeat can be achieved through the development of ^{15}N- and ^{13}C-labeled MUC1 analogues in conjunction with the use of multidimensional NMR methods. Moreover, the study of downstream O-glycosylation events will require the availability of both well-defined glycosylated substrates and soluble recombinant glycosyltransferases (*16*). We report the design and insertion of a synthetic gene coding for a MUC1 polypeptide comprising five tandem repeats into a bacterial expression vector, leading to the production of isotopically labeled forms of this unglycosylated MUC1 analogue. In addition, we report the construction of an expression vector for the production of a soluble form of the most commonly studied human ppGalNAc-transferase, ppGalNAc-T1, in the methyltrophic yeast *Pichia pastoris* (*17*, *18*). More importantly, the availability of ^{15}N- and ^{13}C-labeled MUC1 analogues and of ppGalNAc-T1 allowed us to perform the first high-resolution NMR-based kinetic analysis of the initiating step in the O-glycosylation pathway.

EXPERIMENTAL PROCEDURES

Expression and Purification of MUC1-5TR. A 293-nucleotide double-stranded synthetic gene containing five copies of the MUC1 tandem repeat (MUC1-5TR) with *Escherichia coli* optimized codons and *Nde*I (5′-terminal) and *Bam*HI (3′-terminal) restriction overhangs was synthesized by Midland Certified Reagent Co. (Midland, TX). The gene was inserted at the complementary restriction sites into the pET-15b expression vector (Novagen, Madison, WI), which encodes an N-terminal His_6 metal affinity tag; the primary sequence of the expressed protein is shown in Figure 1A. The resulting construct was used to transform competent *E. coli* BL21(DE3) cells (Novagen). A colony picked from an LB−carbenicillin (50 μg/mL) agar plate was used to inoculate a 40 mL starter culture in LB−carbenicillin medium. This culture was grown overnight at 37 °C with shaking, until turbid, at which point a 20 mL inoculum was transferred to 6 L of prewarmed (37 °C) LB−carbenicillin broth and the incubation was continued until its OD_{600nm} value reached 0.6. Induction of MUC1-5TR was achieved by adding isopropyl β-D-thiogalactopyranoside (IPTG) to a final concentration of 0.5 mM and incubating overnight (14 h) with shaking at 25 °C. Bacterial pellets were recovered by routine centrifugation and MUC1-5TR was purified by IMAC under denaturing conditions. Briefly, bacterial lysates were prepared by stirring the pellets in 5 volumes (100 mL) of lysis buffer (PBS, 8 M urea, and 0.5 M NaCl, pH 7.4) for 2 h at room temperature, then clarified by centrifugation at 15000*g* for 30 min, and loaded onto a 5 mL Ni−NTA−agarose (Qiagen, Mississauga, ON, Canada) column pre-equilibrated with lysis buffer containing 10 mM imidazole. The column was washed with 10 column volumes (50 mL) of the equilibration buffer, and pure MUC1-5TR was subsequently eluted with lysis buffer containing 200 mM imidazole. The eluate was dialyzed exhaustively against 20 mM NH_4HCO_3 prior to lyophilization. The purified proteins were stored at −20 °C until use. The protein was purified from *E. coli* cells in high yield (up to 15 mg/L of cell culture) compared to past expression systems that have included the use of baculovirus/*Sf* 9 insect cells (*19*), transient expression in mammalian cells (*20*), and a previous attempt at expression in *E. coli* (*21*). Uniformly isotopically labeled MUC1-5TR proteins were prepared under essentially the same conditions, except that M9 minimal medium (*22*) supplemented with 0.1 mM $CaCl_2$, 1 mM $MgSO_4$, 0.01 mM $FeCl_3$, 2 mg/L thiamin, and 2 mg/L biotin was used for the induction phase. ^{15}N-Labeled protein was prepared by use of 5 g/L glucose and 1 g/L $^{15}NH_4Cl$ (^{15}N, 98%+; Cambridge Isotope Laboratories, Andover, MA) as the respective carbon and nitrogen sources, whereas ^{15}N,^{13}C-labeled material was produced by additionally substituting 2 g/L [U-$^{13}C_6$]-glucose (^{13}C, 99%; Cambridge Isotope Laboratories) as the carbon source.

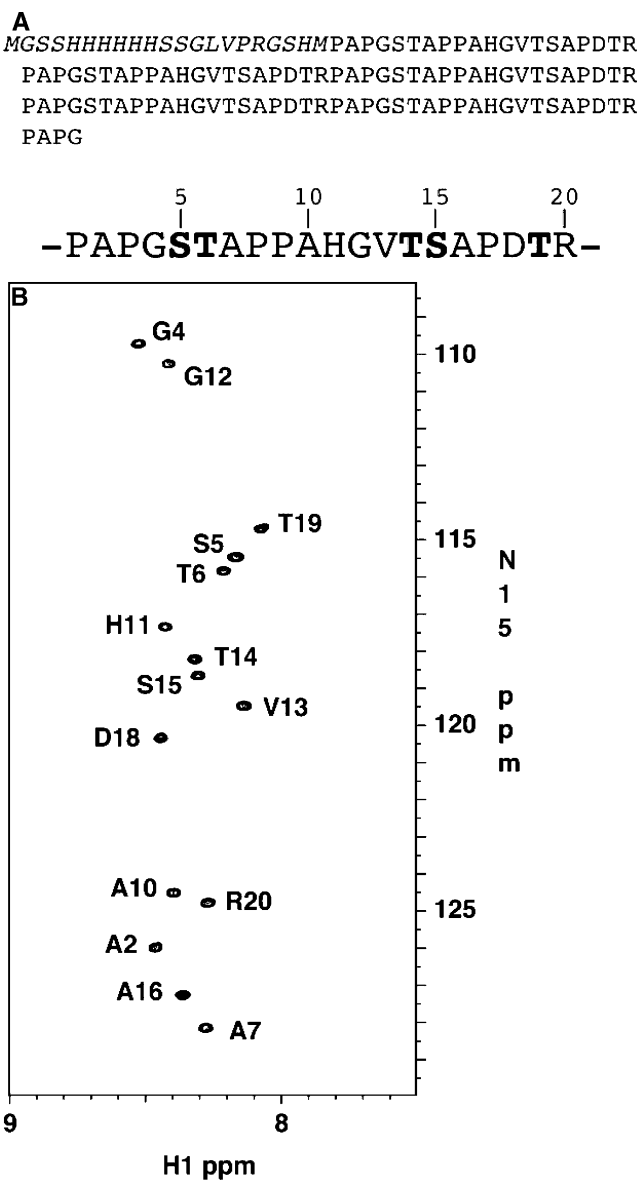

FIGURE 1: Description of a recombinant human mucin MUC1 construct used as a substrate for the human enzyme ppGalNAc-T1. (A) (top) Amino acid sequence of the MUC1-5TR construct. Vector-encoded residues are in italic type. A single MUC1 tandem repeat sequence is shown (bottom), with potential glycosylation sites in boldface type. (B) ^{1}H−^{15}N HSQC spectrum (128 complex t_1 increments of 896 data points, 16 scans) of MUC1-5TR (1.5 mM) in 10 mM sodium phosphate buffer, pH 5.5, 0.01% (w/v) NaN_3, and 10% (v/v) D_2O, 25 °C.

Isotope-labeled MUC1-5TR was purified to homogeneity by the same methods described for unlabeled proteins. Purity of proteins was judged to be at least 95%, as determined by SDS−PAGE and electrospray ionization−mass spectrometry (Molecular Medicine Research Centre Mass Spectrometry Laboratory, University of Toronto).

Expression and Purification of Recombinant ppGalNAc-T1. A search of the public dbEST database of human expressed sequence tags (ESTs) was performed against the ppGalNAc-T1 protein sequence (GenBank Accession No. NP_065207) with the tBLASTx algorithm (http://www.ncbi.nlm.nih.gov/PubMed/blast). Several ESTs were identified and subsequently obtained from the American Type Culture Collection (Manassas, VA). The catalytic domain of the enzyme (amino acids 40−559) was successfully amplified by PCR from clone E3 (IMAGE clone ID 2969475) in two separate reactions with two different primer pairs (reaction 1, 5′-AATTCGGACTTCCTGCTGGAGATGTTCTAGAGCC-3′ and 5′-ACTCAGAATATTTCTGGCAGGGTGACGTTTCG-3′; reaction 2, 5′-CGGACTTCCTGCTGGAGATGTTCTAGAGCC-3′ and 5′-CTAGACTCAGAATATTTCTGGCAGGGTGACGTTTCG-3′). The resulting PCR products were mixed together in an equimolar ratio, denatured at 96 °C for 10 min, and then allowed to reanneal by slow cooling to room temperature. The resulting hybrid duplex was ligated into vector pPICZαA (Invitrogen, Burlington, Ontario) that had been precut with *Eco*RI and *Xba*I. The construct (pPICZα-T1) was isolated following transformation of competent *E. coli* strain DH5α (Invitrogen) and selection on LB−carbenicillin (50 μg mL^{-1}) agar plates, and was verified by sequence analysis of the entire insert region. The recombinant gene product was expressed in *Pichia pastoris* strain KM71H using the EasySelect kit (Invitrogen) in accordance with the manufacturer's protocols. Postinduction media supernatants, containing secreted pp-GalNAc-T1, were concentrated up to 50-fold by ultrafiltration (nominal cutoff 10 kDa) by use of an Amicon stirring unit (Millipore, Etobicoke, Ontario).

NMR Spectroscopy. NMR spectra were recorded on 500 or 600 MHz Varian INOVA spectrometers equipped with a triple-resonance pulse-field gradient probe. Spectra were recorded at 25 °C unless otherwise indicated. ^{1}H−^{15}N heteronuclear single quantum coherence (HSQC) spectra were recorded with 128 and 448 complex points in t_1 and t_2, respectively, unless otherwise stated. Resonance assignments for backbone ^{1}H, $^{13}C_{\alpha}$, $^{13}C_{\beta}$, and ^{15}N nuclei were derived from three-dimensional (3D) HNCACB and HNCOCACB experiments (*23*) of a ^{13}C,^{15}N-labeled sample. Side-chain resonances were assigned by use of 3D ^{15}N-edited TOCSY−HSQC (50 ms mixing time) and NOESY−HSQC (150−320 ms mixing times) data sets. Sweep widths used for acquiring NMR data were 11.7, 20, and 52 ppm for ^{1}H, ^{15}N, and ^{13}C nuclei, respectively. NMR data were processed and analyzed by use of NMRPipe/NMRDraw (*24*) and Xeasy (*25*). The secondary structures of MUC1-5TR and $GalNAc_3$-MUC1-5TR were analyzed by calculating chemical shift indices (CSI) with the weighted function (*26*, *27*) $CSI(C\alpha,C\beta) = [(\Delta C\alpha_{i-1} + \Delta C\beta_{i-1}) + 2(\Delta C\alpha i_i + \Delta C\beta_i) + (\Delta C\alpha_{i+1} + \Delta C\beta_{i+1})]/4$, where $\Delta C\alpha$ and $\Delta C\beta$ correspond to the deviation in parts per million of Cα and Cβ chemical shift values, respectively, from random coil values for the same residue type.

Enzyme Radioassay. The enzymatic activity of recombinant ppGalNAc-T1 was assayed under standard conditions by incubating the appropriate enzyme preparations (typically 1−5 μL of media concentrate, or 0.5−2.5 μg of total protein) at 37 °C with 10 mM $MnCl_2$, 0.7 mM UDP-[1-^{3}H(N)]-*N*-acetylgalactosamine (3.8 mCi/ mmol), 25 mM MES buffer, pH 6.5, 3 mM AMP, and 50 mM GalNAc adjusted to a final volume of 25 μL. A donor substrate concentration of 10 mM UDP-GalNAc was used for determining kinetic parameters. Incubations were performed for 1−15 min and quenched by the addition of 1 mL of ice-cold ddH_2O, prior to solid-phase extraction by a Sep-Pak method as described previously (*28*). In the case of reactions with MUC1-5TR, samples were rebuffered with 0.5 mL of buffer A [30 mM imidazole, 0.9 M NaCl, 150 mM sodium phosphate, and 0.15% (v/v) polyoxyethylene−sorbitan monolaurate (Tween-20), pH 8.0] and the protein was captured by use of 20 μL of magnetic nickel−agarose beads (Qiagen). The beads were washed twice with 0.2 mL of buffer B [20 mM imidazole, 0.3 M NaCl, 50 mM sodium phosphate, and 0.05% (v/v) Tween-20, pH 8.0] and eluted in 50 μL of buffer C [250 mM imidazole, 0.3 M NaCl, 50 mM sodium phosphate, and 0.05% (v/v) Tween-20, pH 8.0]. The level of incorporation of radiolabeled monosaccharides was determined by scintillation counting (2 mL Ultima Gold scintillation fluid; Beckman LS6500 multipurpose scintillation counter).

NMR Glycosylation Assay. Glycosylation of ^{15}N-labeled MUC1-5TR by recombinant ppGalNAc-T1 was monitored by collecting a series of ^{1}H−^{15}N HSQC experiments on a Varian Inova 500 MHz spectrometer. Samples contained 0.4 mM MUC1-5TR, 10 mM UDP-GalNAc, 10 mM MES, pH 6.3, 1 mM $MnCl_2$, 10 mM $MgCl_2$, 0.01% (w/v) NaN_3, and 1% (v/v) ppGalNAc-T1 concentrate in a final volume of 0.6 mL. The time for each experiment was approximately 28 min, and the assay consisted of 32 successive HSQC experiments, with a total time of approximately 15 h. Spectra were processed with the NMRPipe software (*24*) and peaks were picked with NMRDraw. Glycosylation of individual residues by ppGalNAc-T1 were represented graphically by plotting the ratio of the peak volumes for glycosylated residues to the total volume of peaks for both glycosylated and unglycosylated forms versus time elapsed at the midpoint of the spectrum.

Enzyme-Linked Immunosorbent Assays. For ELISA experiments, bovine submaxillary mucin (BSM), bovine serum albumin (BSA), Tween-20, and anti-mouse IgG (whole molecule)−peroxidase were obtained from Sigma−Aldrich (Oakville, ON, Canada). The monoclonal anti-MUC1 antibody *Onc*M27 (*29*) was purified from cultured hybridoma cells by GammaBind Plus Sepharose (Pharmacia, Baie d'Urfé, QC, Canada) according to the manufacturer's instructions, and the monoclonal antibody CC49 (*30*) was a gift from the laboratory of Dr. Raymond Reilly (Faculty of Pharmacy, University of Toronto). MUC1-5TR, $GalNAc_3$-MUC1-5TR, or BSM was dissolved in coating buffer [50 mM $NaHCO_3$ and 0.02% (w/v) NaN_3, pH 9.5] and coated at 4 °C overnight onto Costar 96-well flat-bottom high-binding polystyrene plates (Corning; Corning, NY) at 2 μg (20 μg/mL) per well. The wells were then blocked at room temperature with 100 μL of blocking buffer [PBS, 0.5% (w/v) BSA, and 0.5% (v/v) Tween-20] for 1 h and then incubated sequentially at room temperature for 1 h with 1

Table 1: NMR Assignments for **A**, MUC1-5TR, and **B**, $GalNAc_3$-MUC1-5TR in 10 MM Na-phosphate Buffer, pH 5.5, 0.01 % W/v NaN_3, 10 % V/v D_2O, 25 °C

aa	N	NH	C_α	H_α	C_β	H_β
			(A) MUC1-5TR			
Pro1			62.9	4.4	32.1	2.24, 2.01
Ala2	126	8.46	50.3	4.6	18.2	1.36
Pro3			63.4	4.4	32	2.29, 2.06
Gly4	109.8	8.53	45.4	3.97		
Ser5	115.5	8.17	58.5	4.53	64	3.89
Thr6	116.1	8.22	61.4	4.35	69.9	4.21
Ala7	128.3	8.28	50.5	4.6	18.3	1.35
Pro8				4.38		2.03
Pro9			62.9	4.37	37.9	2.26, 2.01
Ala10	124.7	8.39	52.5	4.23	19.2	1.32
His11	117.4	8.43	55.1	4.69	29.4	3.23
Gly12	110.3	8.42	45.2	3.97		
Val13	119.4	8.14	62.3	4.21	32.8	2.1
Thr14	118.3	8.33	61.7	4.4	69.9	4.23
Ser15	118.7	8.3	58	4.45	63.4	3.84
Ala16	127.3	8.36	50.8	4.64	18.3	1.37
Pro17			63.4	4.4	32.1	2.29, 2.01
Asp18	120.4	8.44	54.2	4.63	41.1	2.69
Thr19	114.7	8.07	61.8	4.31	69.7	4.29
Arg20	124.7	8.27	54.2	4.61	30.4	1.75
			(B) $GalNAc_3$-MUC1-5TR			
Pro1			62.8		32	
Ala2	125.8	8.4	50.3	4.4	18.4	1.35
Pro3			63.2		32.2	
Gly4	108.9	8.4	45.1	3.97		
Ser5	115.9	8.36	56.1	4.78	70.2	4.02, 3.84
Thr6	113.6	8.78	59.5	4.57	79.1	
Ala7	125.4	8.33	50.3	4.4	18.2	1.35
Pro8						
Pro9			62.9		31.9	
Ala10	124.7	8.38	52.4	4.35	19.3	1.3
His11	117.3	8.42	55.3	4.77	29.4	3.19
Gly12	110.0	8.4	45.3	3.94		
Val13	120.1	8.1	62.3	4.28	32.9	2.08
Thr14	117	8.58	59.8	4.66	79.4	
Ser15	116.5	8.47	57.8	4.63	64.3	3.81
Ala16	126.2	8.47	50.6	4.49	18.1	1.39
Pro17			63.2		32	
Asp18	120.5	8.46	54.2	4.66	41.1	2.68
Thr19	114.6	8.07	61.6	4.28	69.7	
Arg20	124.7	8.29	54.2	4.58	30.1	1.75

μg of primary antibody (*Onc*M27 or CC49 at 10 μg/mL in blocking buffer), followed by anti-mouse IgG−peroxidase conjugate (1:1000 dilution in blocking buffer). The plates were developed with 3,3′,5,5′- tetramethylbenzidine (TMB) as the colorimetric substrate (*31*).

RESULTS

Design, Expression, and NMR Characterization of MUC1-5TR. A synthetic gene encoding five tandem repeats from the human mucin MUC1 was cloned into the bacterial expression vector pET-15b (Novagen, Madison, WI), resulting in the overexpression of the MUC1-5TR protein (Figure 1A). The vector-encoded hexahistidinyl (His_6-) tag positioned at the *N*-terminus of the MUC1-5TR construct simplified the recovery of both unglycosylated and glycosylated forms of the construct. Most notably, the bacterial expression system facilitated the production of ^{15}N- and ^{13}C-labeled forms of MUC1-5TR and, in conjunction with multidimensional NMR experiments, resulted in the detailed mapping of all residues within the tandem repeat. Previous NMR structural studies of the MUC1 tandem repeat (*32*−*35*) made use of synthetic peptides and were confined to homonuclear

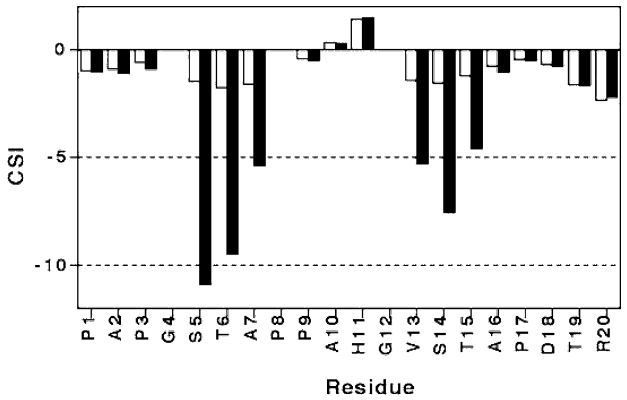

FIGURE 2: Chemical shift index (CSI) (*26*, *27*) for the MUC1 tandem repeat: (open bars) MUC1-5TR and (solid bars) $GalNAc_3$-MUC1-5TR. Four or more consecutive negative CSI values indicate a β-strand, while CSI values near zero indicate random coil sequences.

proton spectra. The $^1H-^{15}N$ HSQC spectrum of unglycosylated ^{15}N-MUC1-5TR at pH 5.5 and 25 °C is shown in Figure 1B. There are only 15 major peaks in the spectrum, corresponding to all the nonproline residues of the tandem repeat. Each peak is a single, sharp resonance, demonstrating that the structure of each repeat is identical within the context of MUC1-5TR. Proton resonances all occur within a narrow chemical shift window (8.0−8.5 ppm), indicative of a random coil-like structure. ^{15}N chemical shift values are also supportive of a random coil peptide (*36*). Backbone ^1H, $^{13}C_\alpha$, ^{15}N, and $^{13}C_\beta$ resonances were assigned by use of 3D-HNCACB and -HN(CO)CACB data sets recorded on ^{13}C-, ^{15}N-labeled MUC1-5TR samples (data not shown). Chemical shift assignments for MUC1-5TR are presented in Table 1A. ^{15}N- and ^{13}C-,^{15}N-edited NOESY experiments at mixing times of 150−320 ms (data not shown), however, did not produce sufficient long-range nuclear Overhauser effects to calculate a unique solution structure for unglycosylated MUC1-5TR. Chemical shift indices (CSI) calculated for each residue are shown in Figure 2. A preponderance of negative values indicates a predominance of β-strand-like structures for the tandem repeat. Interestingly, the highest negative CSI values are for Arg20 and Thr19, two residues present in the immunodominant region of the tandem repeat. Thr19 represents one of the five potential O-glycosylation sites within the MUC1 tandem repeat. This finding suggests the presence of a regular element of secondary structure within this area of the MUC1 tandem repeat. Previous reports proposed the existence of a "knoblike" structure around the APDTR peptide epitope (*32*, *34*). However, the relatively small CSI values (Figure 2) indicate an overall lack of secondary structure for MUC1-5TR, such that this molecule predominantly adopts a more flexible, random coil-like conformation.

Expression and Characterization of a Soluble Form of ppGalNAc-T1. The segment of the human ppGalNAc-T1 gene (*GALNT1*, GenBank Accession No. NM_020474) coding for the soluble catalytic portion (residues 41−559) of the enzyme was amplified by PCR and cloned into the *Pichia pastoris* expression vector pPICZαA. The secreted expression product was a 521-amino acid protein of predicted molecular mass 59.7 kDa, comprising amino acids 41−559 of ppGalNAc-T1 preceded by a vector-encoded EF dipeptide. SDS−PAGE analysis of yeast supernatant fractions yielded only two bands, with apparent molecular masses of 56 and

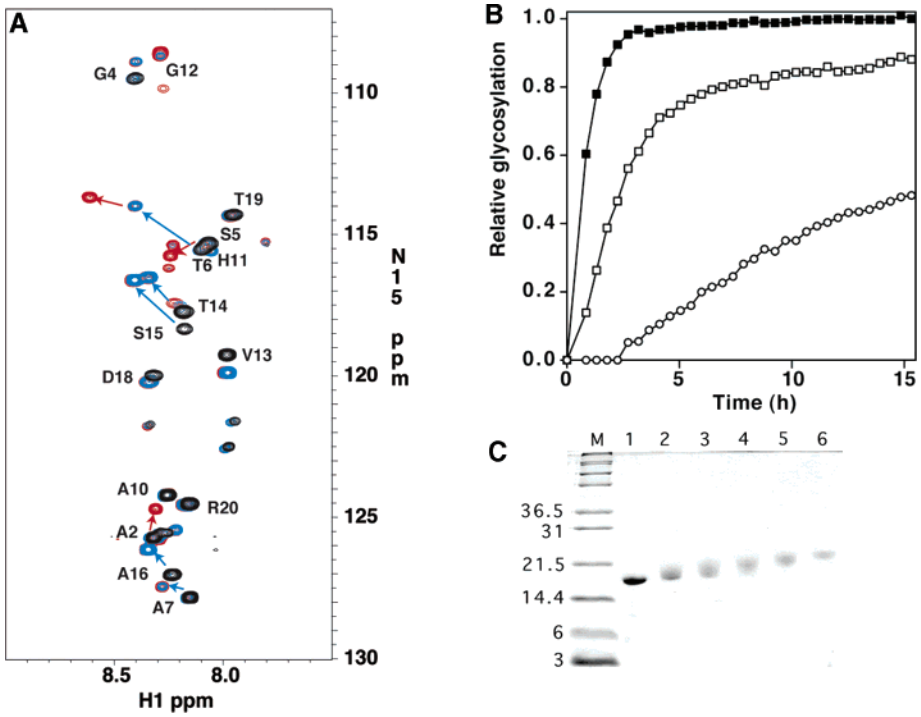

FIGURE 3: Glycosylation of MUC1-5TR by ppGalNAc-T1. (A) $^{1}H-^{15}N$ HSQC spectrum (92 complex t_1 increments of 768 data points, 8 scans) of MUC1-5TR [0.4 mM, in 50 mM UDP-GalNAc, 10 mM MES, pH 6.3, 1 mM $MnCl_2$, 10 mM $MgCl_2$, 0.01% (w/v) NaN_3, and 10% (v/v) D_2O] at (black) 0 h, (blue) 2 h, and (red) 16 h after addition of 1% (v/v) ppGalNAc-T1 preparation. Arrows indicate peak shifts that occur as a result of GalNAc additions to the MUC1 tandem repeat. Unlabeled peaks arise from the vector-encoded His_6 metal affinity tag. Spectra were recorded at 37 °C. (B) Relative glycosylation of MUC1-5TR over time. Values were determined for each residue by analyzing $^{1}H-^{15}N$ HSQC spectra (panel A) and calculating peak volumes for glycosylated and nonglycosylated residues. Relative glycosylation values were defined as the ratio of the volume of the glycosylated peak to the total volume of glycosylated and nonglycosylated peaks. Symbols are as follows: (○) Ser5, (□) Thr6, (■) Thr14. (C) A 20% (w/v) Tris−glycine SDS−PAGE gel of MUC1-5TR protein shown over the time course of glycosylation. Lanes: M, molecular mass standards (indicated in kilodaltons); 1, 0 h; 2, 1 h; 3, 2 h; 4, 4 h; 5, 8 h; and 6, 24 h post-enzyme addition. Incubation was at 37 °C, with 0.4 mM MUC1-5TR, 25 mM MES, pH 6.3, 1 mM $MnCl_2$, 10 mM $MgCl_2$, and 10 mM UDP-GalNAc.

Table 2: Kinetic Parameters of the Recombinant Human ppGalNAc-T1 Enzyme[a]

substrate	V_{max} (μM min^{-1})	acceptor substrate K_m (mM)		
		Ser5	Thr6	Thr14
TAP24	25.7	ND[b]	ND	0.14
MUC1-5TR	28.2	*8.27*	*1.25*	0.04
MUC1-1TR[c]	ND	*41.35*	*6.24*	*0.20*

[a] Interpolated values, italicized, are calculated under the assumption of saturation kinetics. [b] ND, not determined. [c] Parameters for one MUC1 tandem repeat of MUC1-5TR, assuming equivalency for all tandem repeats.

62 kDa. *N*-Terminal Edman degradation on both bands confirmed the presence of the expected target protein and of a truncated form of ppGalNAc-T1 fragment (amino acids 88−559, predicted molecular mass 54.1 kDa). The 62 kDa band was the dominant species, accounting for more than 75% of the total protein as measured by gel densitometry. The recombinant enzyme preparation displayed the expected kinetic parameters as determined by standard radioassays with tritiated UDP-GalNAc as the donor substrate (*28*) and both TAP24 (a 24-amino acid peptide mimic of the MUC1 tandem repeat) and MUC1-5TR as acceptor substrates (see Table 2).

Monitoring the Site-Specific Glycosylation of MUC1-5TR by ppGalNAc-T1 by Use of NMR Spectroscopy. Heteronuclear NMR experiments performed on isotopically labeled forms of the MUC1-5TR construct represent a powerful strategy for simultaneously analyzing the enzymatic action of ppGalNAc-T1 at all five O-glycosylation sites of the tandem repeat. Figure 3A shows the $^{1}H-^{15}N$ HSQC of uniformly ^{15}N-labeled MUC1-5TR (0.4 mM; with 10 mM UDP-GalNAc, 10 mM MES pH 6.3, 1 mM $MnCl_2$, and 10 mM $MgCl_2$) at 0, 2, and 16 h following the addition of the ppGalNAc-T1 preparation. This enzyme has an absolute requirement for paramagnetic Mn^{2+} ions (*13*, *37*). The manganese ions present in the sample (1 mM) result in only minor changes in these spectra relative to those shown in Figure 1B. Ten millimolar Mg^{2+} was also added as a counterion for the UDP-GalNAc donor substrate, ensuring that Mn^{2+} ions remained bound to the enzyme. A change in the chemical shift of His11 is also observed, due to the difference in pH between the ppGalNAc-T1-containing NMR sample (optimal enzymatic activity at pH 6.3) and the sample originally used to establish chemical shift values (pH 5.5; Figure 1B).

The shifts observed in the spectra recorded at 2 and 16 h post-addition of ppGalNAc-T1 are the result of enzyme-catalyzed GalNAc transfer to Ser and Thr residues within MUC1-5TR. Among potential O-glycosylation sites, changes in the ^{15}N and ^{1}H chemical shifts are first observed for Thr14, indicating that it is the sole initial site of O-glycosylation. In the 2 h spectrum, chemical shift changes are also observed for other residues, including movement of the Thr6 resonance, demonstrating that this residue is the second O-glycosylation site. Addition of the GalNAc moiety to Thr6

is virtually complete in the 16 h spectrum; at which time a new peak is arising for Ser5, indicating the commencement of a third O-glycosylation event. Throughout the experiment, the resonance peak assigned to Thr19, a residue located within the immunogenic APDTRP peptide epitope, remains unchanged, confirming that this residue is not glycosylated by ppGalNAc-T1. Significant changes in the chemical shifts of neighboring residues are also noted as a result of O-glycosylation (e.g., Ser15 due to O-glycosylation at Thr14, Ala7 due to Thr6, GalNAc-Thr6 due to Ser5), indicating a change of chemical and structural environments of the tandem repeat peptide due to the presence of GalNAc sugars. The possibility of Ser15 as a potentially O-glycosylated residue itself was ruled out by analysis of its $^{13}C\beta$ chemical shift, which was relatively unaffected after complete glycosylation (Table 1). Thus, the effects on the NH chemical shifts of Ser15 as a result of glycosylation are due to the effects of glycosylation of its neighboring residue, Thr14.

Peak volumes were calculated for each HSQC spectrum acquired during the NMR glycosylation assay and then peaks for O-glycosylated residues were normalized relative to completeness. Figure 3B depicts the O-glycosylation time courses for Ser5, Thr6, and Thr14. The attachment of a GalNAc group to the hydroxyl oxygen of Thr14 is essentially complete within 4 h under the cited experimental conditions. Initial rates of GalNAc addition to the MUC1 construct by ppGalNAc-T1 were derived for each residue from the curves presented in Figure 3B. The overall initial rate of GalNAc transfer to Thr14 was calculated to be 25 μM/min, corresponding to a specific activity of 5.2 units/mg in the stock enzyme preparation (a unit is defined as the transfer of 1 μmol of sugar/min). Similarly, the site-specific initial rates of O-glycosylation at Thr6 and Ser5 were determined to be 8.6 μM/min and 1.7 μM/min, respectively. The initial k_{cat} value of the enzyme (i.e., for Thr14) was estimated at 5.6 s^{-1} with a corresponding k_{cat}/K_m ratio of 1.4×10^5. A large excess of UDP-GalNAc was used in the glycosylation experiments to ensure that product inhibition by UDP was minimized until late time points (>20 h). As with other preparative enzymatic glycosylations (*38*), such inhibition may be countered by phosphatases such as calf intestinal phosphatase (CIP). Experimentally, however, the addition of CIP did not change the glycosylation rates observed (data not shown), presumably owing to the nonoptimal activity of this enzyme under the neutral conditions required for glycosyl transfer (pH 6.5).

The time-dependent addition of GalNAc groups by pp-GalNAc-T1 to MUC1-5TR was also monitored by SDS−PAGE under the same conditions chosen for the NMR experiment (Figure 3C). A single band-shift pattern to a higher mass was clearly observed for the recombinant MUC1-5TR analogue as a result of the enzymatic O-glycosylation of the tandem repeat. Samples taken over a time course (lanes 2−6) displayed the expected pattern of increasing carbohydrate content. Moreover, the band corresponding to the MUC1-5TR substrate became progressively more diffuse within the first 8 h (lanes 2−5), characteristic of glycosylation microheterogeneity, whereas after 24 h the band sharpened once more (lane 6), indicating that MUC1-5TR is terminally O-glycosylated by this time point. The extended structure of the proline-rich tandem repeat and the high level of hydration of the carbohydrate moieties may explain the higher apparent molecular masses calculated from the gel mobility pattern for both unglycosylated (~18 kDa, lane 1) and glycosylated (~30 kDa, lane 6) forms of the MUC1-5TR when compared to their theoretical values (12.0 and 15.0 kDa, respectively).

Characterization of GalNAc$_3$-MUC1-5TR. The curves presented in Figure 3B indicate that O-glycosylation of the MUC1-5TR substrate by the soluble form of ppGalNAc-T1 is essentially complete after 43 h under the conditions of the NMR experiments. The band pattern observed by SDS−PAGE (Figure 3C) also demonstrates that prolonged (24 h) incubation of MUC1-5TR with the enzyme yields a singular glycoform product. A homogeneous preparation of this O-glycosylated substrate, termed GalNAc$_3$-MUC1-5TR, was recovered by immobilized metal affinity chromatography (IMAC) via the N-terminal His_6-tag of the MUC1-5TR construct. The presence of peptide-linked GalNAc groups (constituting the Tn antigen) on purified GalNAc$_3$-MUC1-5TR was then confirmed by ELISA (Figure 4A). The MUC1-specific murine monoclonal antibody (mAb) *Onc*M27 (*29*) recognizes the PDTR peptide sequence within the MUC1 tandem repeat (as defined by peptide scanning; D. Singh, K. Kawamura, and J. Gariépy, unpublished results). This antibody reacted with equal signal intensity to either MUC1-5TR or GalNAc$_3$-MUC1-5TR, confirming that Thr19, the threonine residue within the immunodominant APDTRP region, was not glycosylated by ppGalNAc-T1. As expected, *Onc*M27 did not react with bovine submaxillary mucin (BSM), a highly O-glycosylated mucin that does not contain a PDTR epitope (but that is rich in sialyl-Tn antigens; see below). In contrast, the mouse monoclonal antibody CC49 (*30*), which recognizes both Tn [GalNAc(α1-*O*)Ser/Thr] and sialyl-Tn [Neu5Ac(α2−6)GalNAc(α1-*O*)Ser/Thr] antigens, did not react with MUC1-5TR but did recognize GalNAc$_3$-MUC1-5TR (Tn antigen) and, more strongly, the sialylated glycoprotein BSM (sialyl-Tn). The binding of mAb CC49 to GalNAc$_3$-MUC1-5TR demonstrates that this antibody does indeed cross-react with the Tn antigen, as previously reported (*39*).

The $^1H-^{15}N$ HSQC spectrum of GalNAc$_3$-MUC1-5TR at pH 5.5 and 25 °C is presented in Figure 4B and the resulting NMR chemical shifts for GalNAc$_3$-MUC1-5TR are listed in Table 1B. Assignments of backbone ^{15}N and ^{13}C resonances were also completed for the GalNAc$_3$-MUC1-5TR glycopeptide. The effects of O-glycosylation on MUC1-5TR (Figure 4C) appear to be confined to the immediate vicinity of the O-glycosylated residues, as illustrated by the chemical shift differences (Δ_{av}; Figure 4C) observed for C_α and C_β resonances between GalNAc$_3$-MUC1-5TR and unglycosylated MUC1-5TR. These findings are also confirmed by CSI values for GalNAc$_3$-MUC1-5TR, which remain unchanged from MUC1-5TR (Figure 2), except for those corresponding to the *O*-glycosylated residues and their immediate neighbors (i.e., residues 5−7, 13−15). Amide chemical shift differences (Figure 4D), however, point to significant changes to many residues as a result of O-glycosylation. The large effects observed in NH chemical shifts as a result of GalNAc addition show that simple HSQC spectra, of ^{15}N-labeled proteins, can be used to monitor the substrate specificity of O-glycosylation of mucin proteins by ppGalNAc-transferases, and thus can potentially serve as a tool for examining the

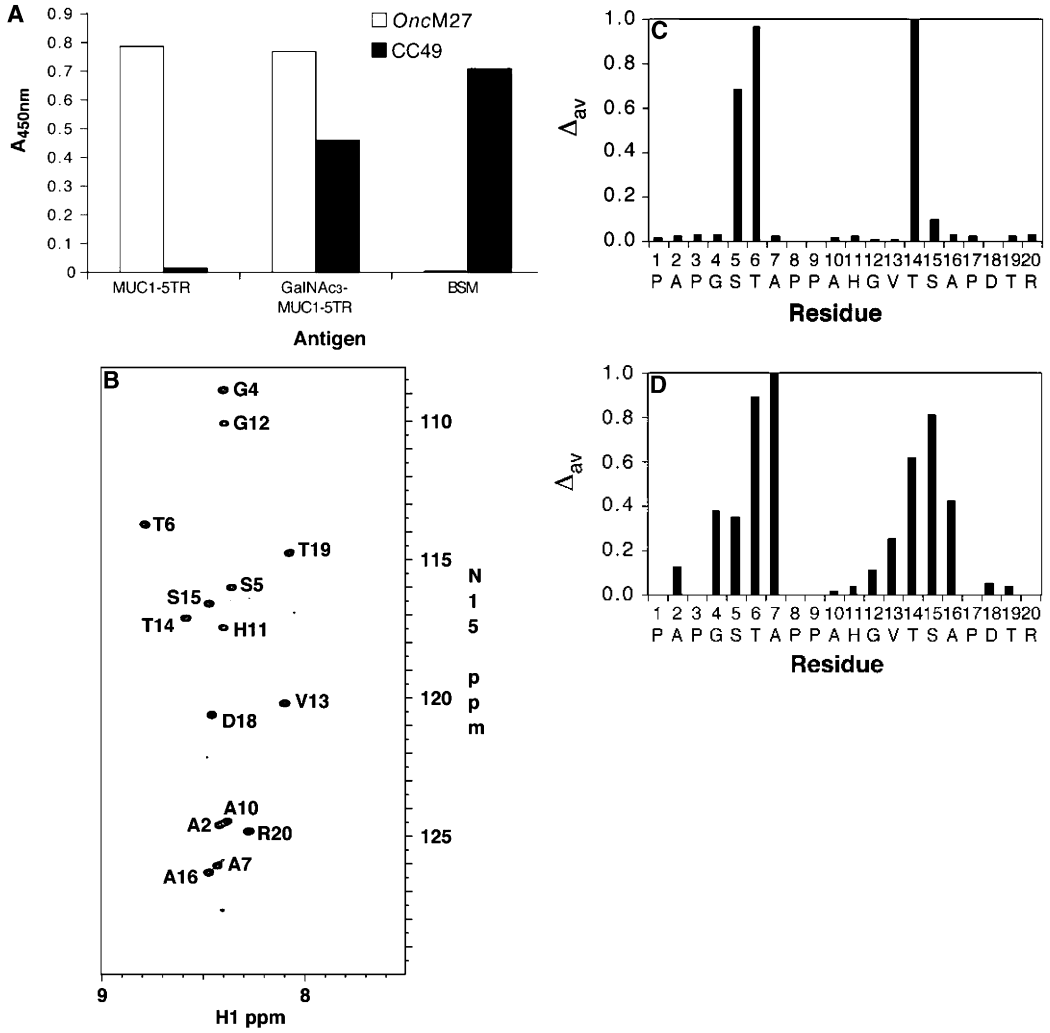

FIGURE 4: Characterization of $GalNAc_3$-MUC1-5TR. (A) ELISA assay of MUC1-5TR, $GalNAc_3$-MUC1-5TR, and bovine submaxillary mucin (BSM) with the monoclonal antibodies (open bars) *Onc*M27 and (solid bars) CC49. Each well was coated with 2 μg of antigen, and 1 μg of primary antibody was used in each case. Color was developed as described in the Experimental Procedures section. (B) $^1H-^{15}N$ HSQC spectrum of $GalNAc_3$-MUC1-5TR (0.5 mM). Experimental parameters and sample conditions are as described for Figure 1B. (C) Normalized C_α/C_β chemical shift differences (Δ_{av}/Δ_{max}) (*49*) as a result of the addition of GalNAc groups on the MUC1 tandem repeat. (D) Normalized amide proton and nitrogen differences.

activities of other glycosyltransferases, either in purified form or as cellular extracts.

DISCUSSION

A complete understanding of how proteins are posttranslationally modified with O-linked sugars requires the detailed knowledge of how transferase enzymes initially differentiate serine and threonine side chains within the context of complex protein templates. The present study provides the first simultaneous kinetic description of O-glycosylation events by ppGalNAc-T1 at all putative O-glycosylation sites within MUC1-5TR. It illustrates the power of NMR spectroscopy for dissecting the substrate specificity and kinetic parameters of a ppGalNAc-transferase in the context of a complex, multivalent MUC1 analogue. More specifically, a synthetic human mucin MUC1 construct harboring five 20-amino acid-long tandem repeats and an N-terminal histidine purification tag was expressed in bacteria and subsequently O-glycosylated with a soluble catalytic fragment (amino acids 41−559) of human ppGalNAc-T1 (Figure 1). The order of addition of GalNAc moieties (creating the Tn antigen) is sequential and specifically occurred at only three of the five hydroxyamino acid side chains within the tandem repeat. Thr14 represented the best substrate for this enzyme, followed by Thr6. The ppGalNAc-T1 enzyme subsequently slowly modifies Ser5 after a 2-h "lag period," during which time most of the Thr14 (> 90%; Figure 3B) and Thr6 side chains (~60%) are glycosylated, suggesting that the enzyme may have a secondary specificity for altered substrates (glycosylated forms). This delay between the successive engagement of the different O-glycosylation sites by the enzyme may thus support the proposed functional lectinlike properties of ppGalNac-T1 (*40*). Both Ser15 and Thr19 are not substrates for this enzyme. Surprisingly, these two residues, particularly Thr19, are part of a region of the unglycosylated MUC1-5TR that display the only ordered or "knoblike" structure within the MUC1 tandem repeat (Figure 2; *30*, *32*). The substrate selectivity of ppGalNac-T1 thus appears to favor residues located in regions of the unglycosylated MUC1-5TR lacking elements of secondary structure and perhaps better defined as a "loose extended" structure reflecting its high content of proline residues.

The structural effects of O-glycosylation on MUC1-5TR, as determined by NMR studies, were limited to the vicinity

of the glycosylated residues. Interestingly, the scale at which the resulting ^{15}N,^{13}C-labeled-glycopeptide GalNAc$_3$-MUC1-5TR could be produced and purified demonstrates the value of this glycosylated substrate for further dissecting the features of other enzymes involved in O-glycosylation. Other members of the ppGalNAc-transferase family for example, exhibit a strict requirement for glycopeptide substrates, and, in some instances, are capable of completing the O-glycosylation of the MUC1 tandem repeat following the prior action of ppGalNAc-T1 (*41*−*43*). In addition, downstream transferases including the human α2,6-sialyltransferases (*18*, *44*) and the recently cloned core 1 β1,3-galactosyltransferases (*45*, *46*) could be used in conjunction with GalNAc$_3$-MUC1-5TR to recreate cancer-relevant glycopeptide antigens, including sialyl-Tn [Neu5Ac(α2−6)GalNAc(α1-*O*)Ser/Thr], a predominant marker in colon carcinomas (*47*), and sialyl-T [Neu5Ac(α2−3)Gal(β1−3)GalNAc(α1-*O*)-Ser/Thr], frequently observed in breast cancers (*48*). Finally, the strategy presented in this study now provides the tools for collecting structural information essential to the rational design of glycosylated forms of MUC1 that may serve as components in cancer vaccines or as validated targets for drug discovery.

ACKNOWLEDGMENT

We thank Dr. Harry Schachter (Hospital for Sick Children, Toronto) for insightful discussion and assistance with enzyme radioassays.

REFERENCES

1. Elhammer, A. P., Kezdy, F. J., and Kurosaka, A. (1999) The acceptor specificity of UDP-GalNAc:polypeptide *N*- acetylgalactosaminyltransferases, *Glycoconjugate J. 16*, 171−80.
2. Wang, H., Tachibana, K., Zhang, Y., Iwasaki, H., Kameyama, A., Cheng, L., Guo, J., Hiruma, T., Togayachi, A., Kudo, T., Kikuchi, N., and Narimatsu, H. (2003) Cloning and characterization of a novel UDP-GalNAc:polypeptide *N*-acetylgalactosaminyltransferase, pp-GalNAc-T14, *Biochem. Biophys Res. Commun. 300*, 738−44.
3. Kingsley, P. D., Hagen, K. G., Maltby, K. M., Zara, J., and Tabak, L. A. (2000) Diverse spatial expression patterns of UDP-GalNAc: polypeptide *N*-acetylgalactosaminyltransferase family member mRNAs during mouse development, *Glycobiology 10*, 1317−23.
4. Hanisch, F. G., and Muller, S. (2000) MUC1: the polymorphic appearance of a human mucin, *Glycobiology 10*, 439−49.
5. Gendler, S. J. (2001) MUC1, the renaissance molecule, *J. Mammary Gland Biol. Neoplasia 6*, 339−53.
6. Taylor-Papadimitriou, J., Burchell, J. M., Plunkett, T., Graham, R., Correa, I., Miles, D., and Smith, M. (2002) MUC1 and the immunobiology of cancer, *J. Mammary Gland Biol. Neoplasia 7*, 209−21.
7. Denda-Nagai, K., and Irimura, T. (2000) MUC1 in carcinoma−host interactions, *Glycoconjugate J. 17*, 649−58.
8. Burchell, J. M., Mungul, A., and Taylor-Papadimitriou, J. (2001) O-linked glycosylation in the mammary gland: changes that occur during malignancy, *J. Mammary Gland Biol. Neoplasia 6*, 355−64.
9. Spencer, D. I., Price, M. R., Tendler, S. J., De Matteis, C. I., Stadie, T., and Hanisch, F. G. (1996) Effect of glycosylation of a synthetic MUC1 mucin-core-related peptide on recognition by anti-mucin antibodies, *Cancer Lett. 100*, 11−5.
10. Karsten, U., Diotel, C., Klich, G., Paulsen, H., Goletz, S., Muller, S., and Hanisch, F. G. (1998) Enhanced binding of antibodies to the DTR motif of MUC1 tandem repeat peptide is mediated by site-specific glycosylation, *Cancer Res. 58*, 2541−9.
11. Price, M. R., Rye, P. D., Petrakou, E., Murray, A., Brady, K., Imai, S., Haga, S., Kiyozuka, Y., Schol, D., Meulenbroek, M. F., Snijdewint, F. G., von Mensdorff-Pouilly, S., Verstraeten, R. A., Kenemans, P., Blockzjil, A., Nilsson, K., Nilsson, O., Reddish, M., Suresh, M. R., Koganty, R. R., Fortier, S., Baronic, L., Berg, A., Longenecker, M. B., Hilgers, J., et al. (1998) Summary report on the ISOBM TD-4 Workshop: analysis of 56 monoclonal antibodies against the MUC1 mucin, *Tumour Biol. 19*, 1−20.
12. Syrigos, K. N., Karayiannakis, A. J., and Zbar, A. (1999) Mucins as immunogenic targets in cancer, *Anticancer Res. 19*, 5239−44.
13. Wandall, H. H., Hassan, H., Mirgorodskaya, E., Kristensen, A. K., Roepstorff, P., Bennett, E. P., Nielsen, P. A., Hollingsworth, M. A., Burchell, J., Taylor-Papadimitriou, J., and Clausen, H. (1997) Substrate specificities of three members of the human UDP-*N*-acetyl-α-D-galactosamine:Polypeptide *N*-acetylgalactosaminyltransferase family, GalNAc-T1, -T2, and -T3, *J. Biol. Chem. 272*, 23503−14.
14. Hanisch, F. G., Reis, C. A., Clausen, H., and Paulsen, H. (2001) Evidence for glycosylation-dependent activities of polypeptide *N*-acetylgalactosaminyltransferases rGalNAc-T2 and -T4 on mucin glycopeptides, *Glycobiology 11*, 731−40.
15. Gerken, T. A., Zhang, J., Levine, J., and Elhammer, A. (2002) Mucin core O-glycosylation is modulated by neighboring residue glycosylation status. Kinetic modeling of the site-specific glycosylation of the apo-porcine submaxillary mucin tandem repeat by UDP-GalNAc:polypeptide *N*-acetylgalactosaminyltransferases T1 and T2, *J. Biol. Chem. 277*, 49850−62.
16. Vlad, A. M., Muller, S., Cudic, M., Paulsen, H., Otvos, L., Jr., Hanisch, F. G., and Finn, O. J. (2002) Complex carbohydrates are not removed during processing of glycoproteins by dendritic cells: processing of tumor antigen MUC1 glycopeptides for presentation to major histocompatibility complex class II-restricted T cells, *J. Exp. Med. 196*, 1435−46.
17. Malissard, M., Zeng, S., and Berger, E. G. (1999) The yeast expression system for recombinant glycosyltransferases, *Glycoconjugate J. 16*, 125−39.
18. Malissard, M., Zeng, S., and Berger, E. G. (2000) Expression of functional soluble forms of human beta-1,4-galactosyltransferase I, alpha-2,6-sialyltransferase, and alpha-1,3-fucosyltransferase VI in the methylotrophic yeast *Pichia pastoris*, *Biochem. Biophys. Res. Commun. 267*, 169−73.
19. Soares, M., Hanisch, F. G., Finn, O. J., and Ciborowski, P. (2001) Recombinant human tumor antigen MUC1 expressed in insect cells: structure and immunogenicity, *Protein Expression Purif. 22*, 92−100.
20. Muller, S., and Hanisch, F. G. (2002) Recombinant MUC1 probe authentically reflects cell-specific O-glycosylation profiles of endogenous breast cancer mucin. High density and prevalent core 2-based glycosylation, *J. Biol. Chem. 277*, 26103−12.
21. Dolby, N., Dombrowski, K. E., and Wright, S. E. (1999) Design and expression of a synthetic mucin gene fragment in *Escherichia coli*, *Protein Expression Purif. 15*, 146−54.
22. Sambrook, J., Fritsch, E. F., and Maniatis, T. (1989) *Molecular cloning: A laboratory manual*, 2nd ed., Cold Spring Harbor Laboratory Press, Cold Spring Harbor, NY.
23. Yamazaki, T., Lee, W., Arrowsmith, C. H., Muhandiram, D. R., and Kay, L. E. (1994) Backbone assignment of ^{15}N, ^{13}C, ^{2}H labeled proteins with high sensitivity, *J. Am. Chem. Soc. 116*, 11655−11666.
24. Delaglio, F., Grzesiek, S., Vuister, G. W., Zhu, G., Pfeifer, J., and Bax, A. (1995) NMRPipe: a multidimensional spectral processing system based on UNIX pipes, *J. Biomol. NMR 6*, 277−93.
25. Bartels, C. H., Xia, T.-H., Billeter, M., Güntert, P., and Wüthrich, K. (1995) XEASY for computer-supported NMR spectral-analysis of biological macromolecules, *J. Biomol. NMR 5*, 1−10.
26. Abu-Abed, M., Mal, T. K., Kainosho, M., MacLennan, D. H., and Ikura, M. (2002) Characterization of the ATP-binding domain of the sarco(endo)plasmic reticulum Ca^{2+}-ATPase: probing nucleotide binding by multidimensional NMR, *Biochemistry 41*, 1156−64.
27. Wishart, D. S., and Sykes, B. D. (1994) The ^{13}C chemical-shift index: a simple method for the identification of protein secondary structure using ^{13}C chemical-shift data, *J. Biomol. NMR 4*, 171−180.
28. Brockhausen, I. (2000) O-linked chain glycosyltransferases, *Methods Mol. Biol. 125*, 273−93.
29. Linsley, P. S., Brown, J. P., Magnani, J. L., and Horn, D. (1988) Monoclonal antibodies reactive with mucin glycoproteins found in sera from breast cancer patients, *Cancer Res. 48*, 2138−48.
30. Hanisch, F. G., Uhlenbruck, G., Egge, H., and Peter-Katalinic, J. (1989) A B72.3 second-generation-monoclonal antibody (CC49)

defines the mucin-carried carbohydrate epitope Gal β(1−3)[NeuAc α(2−6)]GalNAc, *Biol. Chem. Hoppe-Seyler 370*, 21−6.
31. Madersbacher, S., and Berger, P. (1991) Double wavelength measurement of 3,3′,5,5′-tetramethylbenzidine (TMB) provides a 3-fold enhancement of the ELISA measuring range, *J. Immunol. Methods 138*, 121−4.
32. Fontenot, J. D., Mariappan, S. V., Catasti, P., Domenech, N., Finn, O. J., and Gupta, G. (1995) Structure of a tumor associated antigen containing a tandemly repeated immunodominant epitope, *J. Biomol. Struct. Dyn. 13*, 245−60.
33. Grinstead, J. S., Koganty, R. R., Krantz, M. J., Longenecker, B. M., and Campbell, A. P. (2002) Effect of glycosylation on MUC1 humoral immune recognition: NMR studies of MUC1 glycopeptide−antibody interactions, *Biochemistry 41*, 9946−61.
34. Kirnarsky, L., Prakash, O., Vogen, S. M., Nomoto, M., Hollingsworth, M. A., and Sherman, S. (2000) Structural effects of O-glycosylation on a 15-residue peptide from the mucin (MUC1) core protein, *Biochemistry 39*, 12076−82.
35. Schuman, J., Campbell, A. P., Koganty, R. R., and Longenecker, B. M. (2003) Probing the conformational and dynamical effects of O-glycosylation within the immunodominant region of a MUC1 peptide tumor antigen, *J. Pept. Res. 61*, 91−108.
36. Wishart, D. S., Sykes, B. D., and Richards, F. M. (1991) Relationship between nuclear magnetic resonance chemical shift and protein secondary structure, *J. Mol. Biol. 222*, 311−33.
37. Unligil, U. M., and Rini, J. M. (2000) Glycosyltransferase structure and mechanism, *Curr. Opin. Struct. Biol. 10*, 510−7.
38. George, S. K., Schwientek, T., Holm, B., Reis, C. A., Clausen, H., and Kihlberg, J. (2001) Chemoenzymatic synthesis of sialylated glycopeptides derived from mucins and T-cell stimulating peptides, *J. Am. Chem. Soc. 123*, 11117−25.
39. Reddish, M. A., Jackson, L., Koganty, R. R., Qiu, D., Hong, W., and Longenecker, B. M. (1997) Specificities of anti-sialyl-Tn and anti-Tn monoclonal antibodies generated using novel clustered synthetic glycopeptide epitopes, *Glycoconjugate J. 14*, 549−60.
40. Tenno, M., Kezdy, F. J., Elhammer, A. P., and Kurosaka, A. (2002) Function of the lectin domain of polypeptide *N*-acetylgalactosaminyltransferase 1, *Biochem. Biophys. Res. Commun. 298*, 755−9.
41. Ten Hagen, K. G., Bedi, G. S., Tetaert, D., Kingsley, P. D., Hagen, F. K., Balys, M. M., Beres, T. M., Degand, P., and Tabak, L. A. (2001) Cloning and characterization of a ninth member of the UDP-GalNAc:polypeptide *N*-acetylgalactosaminyltransferase family, ppGaNTase-T9, *J. Biol. Chem. 276*, 17395−404.
42. Ten Hagen, K. G., Tetaert, D., Hagen, F. K., Richet, C., Beres, T. M., Gagnon, J., Balys, M. M., VanWuyckhuyse, B., Bedi, G. S., Degand, P., and Tabak, L. A. (1999) Characterization of a UDP-GalNAc:polypeptide *N*-acetylgalactosaminyltransferase that displays glycopeptide *N*- acetylgalactosaminyltransferase activity, *J. Biol. Chem. 274*, 27867−74.
43. Bennett, E. P., Hassan, H., Mandel, U., Mirgorodskaya, E., Roepstorff, P., Burchell, J., Taylor-Papadimitriou, J., Hollingsworth, M. A., Merkx, G., van Kessel, A. G., Eiberg, H., Steffensen, R., and Clausen, H. (1998) Cloning of a human UDP-*N*-acetyl-α-D-galactosamine:polypeptide *N*-acetylgalactosaminyltransferase that complements other GalNAc− transferases in complete O-glycosylation of the MUC1 tandem repeat, *J. Biol. Chem. 273*, 30472−81.
44. Chotigeat, W., Chayanunnukul, W., and Phongdara, A. (2000) Expression of a mammalian α2,6-sialyltransferase gene in *Pichia pastoris*, *J. Biotechnol. 81*, 55−61.
45. Ju, T., Brewer, K., D_Souza, A., Cummings, R. D., and Canfield, W. M. (2002) Cloning and expression of human core 1 β1,3-galactosyltransferase, *J. Biol. Chem. 277*, 178−86.
46. Kudo, T., Iwai, T., Kubota, T., Iwasaki, H., Takayma, Y., Hiruma, T., Inaba, N., Zhang, Y., Gotoh, M., Togayachi, A., and Narimatsu, H. (2002) Molecular cloning and characterization of a novel UDP-Gal:GalNAcα peptide β1,3-Galactosyltransferase (C1Gal-T2), an enzyme synthesizing a core 1 structure of O-glycan, *J. Biol. Chem. 277*, 47724−47731.
47. Brockhausen, I., Yang, J., Dickinson, N., Ogata, S., and Itzkowitz, S. H. (1998) Enzymatic basis for sialyl-Tn expression in human colon cancer cells, *Glycoconjugate J. 15*, 595−603.
48. Lloyd, K. O., Burchell, J., Kudryashov, V., Yin, B. W., and Taylor-Papadimitriou, J. (1996) Comparison of O-linked carbohydrate chains in MUC-1 mucin from normal breast epithelial cell lines and breast carcinoma cell lines. Demonstration of simpler and fewer glycan chains in tumor cells, *J. Biol. Chem. 271*, 33325−34.
49. Foster, M. P., Wuttke, D. S., Clemens, K. R., Jahnke, W., Radhakrishnan, I., Tennant, L., Reymond, M., Chung, J., and Wright, P. E. (1998) Chemical shift as a probe of molecular interfaces: NMR studies of DNA binding by the three amino-terminal zinc finger domains from transcription factor IIIA, *J. Biomol. NMR 12*, 51−71.

BI0353070